

## Anomalous Heating of a Plasma by a Laser

C. Yamanaka,\* T. Yamanaka,\* T. Sasaki, K. Yoshida, and M. Waki  
*Faculty of Engineering, Osaka University, Osaka 565, Japan*

and

H. B. Kang  
*Institute of Plasma Physics, Nagoya University, Nagoya 464, Japan*  
 (Received 24 April 1972)

As lasers have an ability to deliver a large amount of energy very rapidly to matter, one can produce a plasma of thermonuclear temperature by laser bombardment of matter. We observed a neutron yield from a solid deuterium target irradiated by the beam of a glass laser, which had a power of 20 GW for 2 nsec. The theoretically estimated threshold laser power for anomalous heating owing to the parametric instability was in agreement with the experimental result. Above this threshold, an increase in the electron temperature, the appearance of a fast-ion group, and an anomaly in the reflection of light from the plasma were observed. These phenomena were closely correlated with the neutron yield. At the high-temperature region above a few hundred electron volts, the anomalous heating plays an essential role in reaching the fusion-reaction temperature.

### I. INTRODUCTION

With the development of high-intensity lasers, one can produce plasmas with high density and high temperature which are relevant to thermonuclear-fusion research.<sup>1</sup> The Limeil group<sup>2</sup> has reported substantial neutron emission from a solid deuterium target irradiated by a 7-nsec 4-GW Nd<sup>3+</sup> laser. (Recently they used a 3.5-nsec 24-GW glass-laser system.)

In order to investigate the potential of laser produced plasma for a future fusion reactor, a detailed investigation of the properties<sup>3</sup> of these plasmas is very important. In particular the laser heating process is one of the most important topics to study. Classical absorption is weak at high temperatures and becomes inefficient as the temperature increases. The absorption length  $l$  near the cutoff density of glass-laser light is

$$l = 5 \times 10^{35} T_e^{3/2} n^{-2} \text{ (cm)},$$

where  $T_e$  is the electron temperature in eV and  $n$  is the density in  $\text{cm}^{-3}$ . For a density of  $10^{21} \text{ cm}^{-3}$  and a temperature of 1 keV, the absorption length is 150  $\mu$ . Therefore the absorption is small within a focal spot of 100  $\mu$  in diameter with a plasma of this temperature and density. According to the classical process, the laser beam would be perfectly reflected or transmitted with very little absorption, depending on whether the laser frequency  $\omega_0$  is less than or greater than the plasma frequency  $\omega_{ep}$ . Considering our experimental results, it seems that anomalous absorption due to nonlinear effects induced by the high field strength of the laser beam is important in heating the plasma.

In this paper we report the properties of laser plasmas from solid deuterium and LiH targets, measured by various kinds of diagnostics, and we discuss the correlation of the neutron yield to the anomalous effects.

### II. EXPERIMENTAL ARRANGEMENT

The laser was composed of an oscillator and five amplifiers<sup>4,5</sup> constructed in our laboratory. Three alternative oscillators could be used. Two of these were glass lasers, operating in the nanosecond and picosecond ranges, respectively. The third was a YAG oscillator which had a narrow spectrum beam especially suitable for scattering spectroscopy. The nanosecond oscillator delivered a pulse whose duration could be varied<sup>6</sup> from 2 to 10 nsec with a rise time of 1 nsec. A pulse-shaping system consisting of a laser-triggered spark gap, a potassium diphosphate (KDP) Pockels cell, and Glan prisms was employed. The oscillator pulse could be amplified up to more than 40 J, corresponding to 20 GW for a 2-nsec pulse. The energy of the pulse was kept below its maximum attainable value as a precaution against damage to the glass lasers by the beam reflected from the target. The damage to the glasses has been completely studied and has been reported elsewhere.<sup>7</sup> To protect the glasses from the reflection, we used a Faraday rotator, dye cells, and a special uniguide slit which was provided with an afocal lens system and a pin-hole slit as shown in Fig. 1. In this system the weak forward laser beam passes through the slit but the more intense backward one produces a plasma at the slit, which prevents the reflected beam passing through the slit. By these methods the reflected beam could be attenuated by

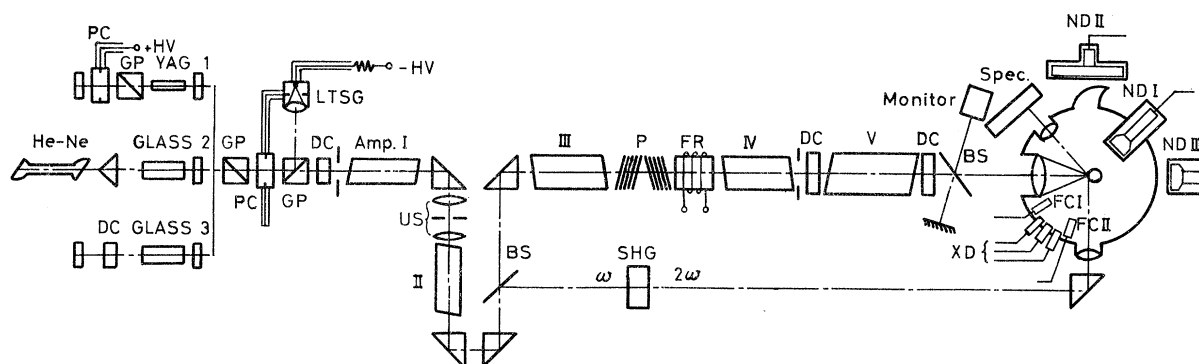


FIG. 1. Experimental arrangement of laser plasma research. 1: Pockels cell Q-switched yttrium-aluminum-garnet (YAG) laser, 2: rotating prism Q-switched glass laser, 3: mode locked glass laser, PC: Pockels cell, DC: saturable dye cell, XD: x-ray detector, ND: neutron detector, FC: Faraday cage, Spec: spectrometer, US: uniguide slit, A: attenuator.

more than a factor of  $10^4$ .

The picosecond oscillator could deliver a single pulse selected from a train of picosecond mode locked pulses by the pulse transmission mode method, which has been described in a previous paper.<sup>3</sup> To amplify the picosecond pulse, a  $\text{POCl}_3\text{-Nd}^{+3}$  liquid<sup>8</sup> laser seemed to be most suitable since it has a larger transition cross section than that of a glass amplifier.

The yttrium-aluminum-garnet (YAG) laser was Q switched by a Pockels cell and fed to the glass preamplifier through the pulse-forming system. Then the beam was separated into two, one of which was used to generate second harmonics of a few MW by a KDP crystal and the other was sent to the main amplifier (see Table I).

The divergence of the output beam was less than 1 mrad. It was focused onto the target using an aspherical lens of focal length 50 mm and  $f=0.83$ .

The experimental arrangement is shown schematically in Fig. 1. A cryostat of liquid helium produced a solid deuterium stick, the diameter of which was 2 mm, in a vacuum of  $10^{-7}$  Torr.

### III. EXPERIMENTAL RESULTS

#### A. Preliminary Results for Laser Plasma

To identify the properties of the plasma that depend on the type of laser target, we performed

experiments on a small suspended particle and on a solid thick plate, each made of LiH. Streak photographs of a LiH particle  $50\ \mu$  in diameter irradiated by a glass-laser beam were taken using an STL streak camera. The expansion velocity was about  $5 \times 10^7$  cm/sec as shown in Fig. 2. At a distance of 30 cm from the irradiated point,  $\text{H}^{1+}$ ,  $\text{Li}^{1+}$ , and  $\text{Li}^{2+}$  ions were resolved by an energy analyzer, and their velocities were found to be  $2.4 \times 10^7$ ,  $2.7 \times 10^7$ , and  $4 \times 10^7$  cm/sec, respectively.<sup>9</sup> This is in agreement with the well-known characteristics<sup>10-14</sup> of multicharged laser plasmas.

From our simple gas-dynamical computation,<sup>15,16</sup> when the glass-laser rise time is 2 nsec and the power is 10 GW, the temperature reaches a maximum of 300 eV within 1 nsec and then decreases. Applying a magnetic field to suppress the expansion, the decrease in the temperature reverses and the temperature can rise again to 600 eV after the expansion. Without a magnetic field, inertial confinement seems to finish after 1 nsec. The experimental values of electron temperature are in good agreement with the calculated values, which are shown in Fig. 3.

When we used a thick target, the plasma formed had some spatial structure<sup>10,17</sup> which was probably caused by the self-induced field.<sup>18</sup> After the appearance of the plasma, very-high-density neutral gas appears. The electron and neutral gas densi-

TABLE I. Parameters of the glass amplifier.

	Osc.	Amp. I	Amp. II	Amp. III	Amp. IV	Amp. V
Rod dimension (mm)	$10^{\phi} \times 150^l$	$20^{\phi} \times 320^l$	$20^{\phi} \times 320^l$	$30^{\phi} \times 320^l$	$30^{\phi} \times 320^l$	$40^{\phi} \times 600^l$
$\text{Nd}_2\text{O}_3$ (wt%)	3.5	3.5	3.5	3.5	3.5	3.5
Flash lamp	2	4	4	6	6	10
Pumping energy (kJ)	0.8	9	9	13.5	13.5	60
Output power (MW)	4.5	31.5	160	720	2900	$10^4$
Gain		7	5	4.5	4	3.5

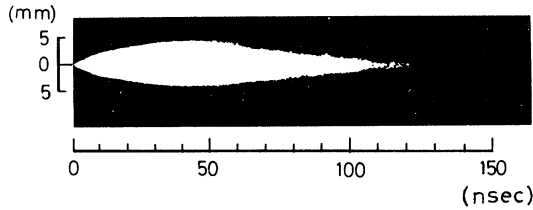


FIG. 2. Streak photograph of suspended LiH particle  $50 \mu$  in diameter irradiated by glass laser.

ties were measured<sup>19</sup> using Thomson and Rayleigh scattering of the laser light as shown in Fig. 4. The appearance of this neutral gas is a drawback for the magnetic confinement of a laser plasma.

### B. Neutron Yield from Deuterium Targets

To investigate the laser-heating process for a deuterium plasma we examined the correlation between the plasma parameters and the neutron yield.

#### 1. Electron Temperature

The electron temperature was measured from the absorption of soft x rays from the plasma by plastic scintillators with beryllium windows of different thickness (25, 50, and  $100 \mu$ ). The small type of photomultiplier HTV-R292 has a time resolution of 10 nsec. The experimental results for solid deuterium are shown in Fig. 5. The laser-pulse<sup>13</sup> duration did not seem to influence the electron temperature for the cases where the duration was 2, 4, and 10 nsec. The dependence of the electron temperature on the laser power seems to have an abrupt change at a power of 2 GW. Below this point the electron temperature had a dependence on laser power  $P$  of  $P^{2/3}$ , while above this point the dependence was  $P^{1.2}$ , and also the data

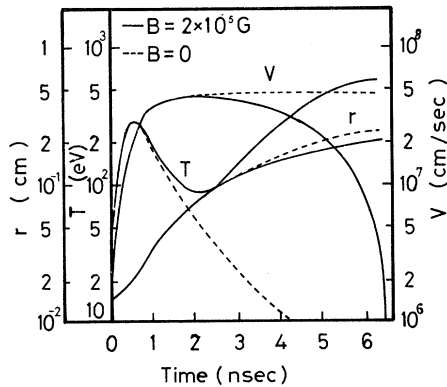


FIG. 3. Gas-dynamical behavior of laser-irradiated LiH particle, laser power: 10 GW, rise time: 2 nsec, focal spot size:  $100 \mu$ , particle size:  $50 \mu$ , magnetic field:  $2 \times 10^5$  G.

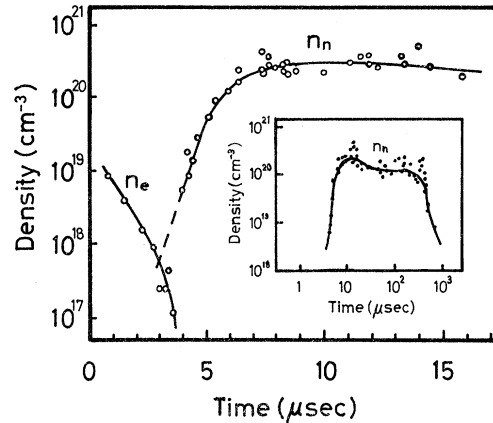


FIG. 4. Evaporation of dense neutral atoms from laser-irradiated solid target measured by light scattering.

began to scatter. The above point of discontinuity corresponded to a laser intensity of about  $10^{13}$  W/cm<sup>2</sup>; this will be referred to as the critical intensity.

#### 2. Laser-Beam Reflection

A fairly large amount of the input laser energy was reflected by the target. The pulse form of the input and reflected laser light was measured by the same biplanar photodiode, type HTV-R317. The ratio of reflected energy to incident energy changed suddenly from 4 to 20% at a laser intensity of  $10^{13}$  W/cm<sup>2</sup>, i. e., at the critical intensity.

At the lower side of this intensity where the electron temperature was about 200 eV, the reflected laser light<sup>20</sup> was often observed to oscillate with a frequency of about  $10^9$  Hz.

#### 3. Ion Collection and Time of Flight

As previously reported,<sup>17,21</sup> the ejection of the laser plasma from the target had some directional dependence. We measured the ion flux at  $30^\circ$  and

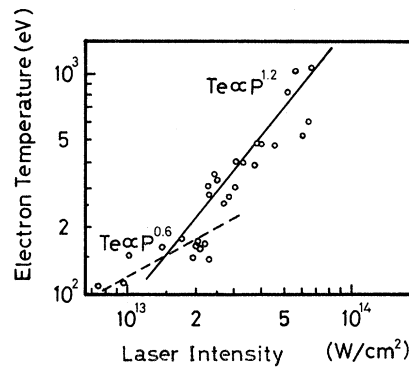


FIG. 5. Dependence of electron temperature of deuterium plasma on incident laser intensity.

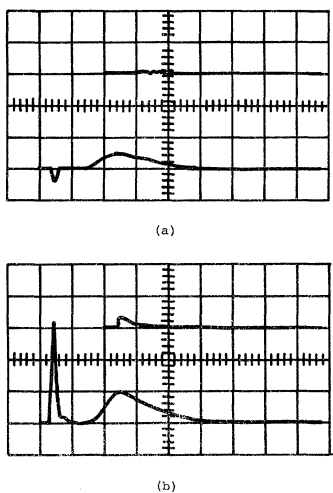


FIG. 6. Time of flight of ions from deuterium solid target. (a) laser power 1.1 GW, (b) laser power 3 GW; sweep time: 200 nsec/division. Upper trace: 60° from the incident beam, lower trace: 30° from the incident beam.

60° to the incident beam as shown in Fig. 6. The time-of-flight measurements showed the existence of two groups of ions, fast and slow, above the critical laser intensity. Below the critical point only the slow-ion component was observed. The dependence of the mean ion velocity  $V_b$  on the electron temperature is shown in Fig. 7. The number of ions in the slow component decreased with the increasing of electron temperature, while the number in the fast component increased as shown in Fig. 8. The ion temperature  $T_i$ <sup>21,22</sup> was estimated from the velocity profiles of the ions, which are shown in Fig. 9. The temperature of the fast component had a dependence on laser power of  $P^{1.2}$ , while

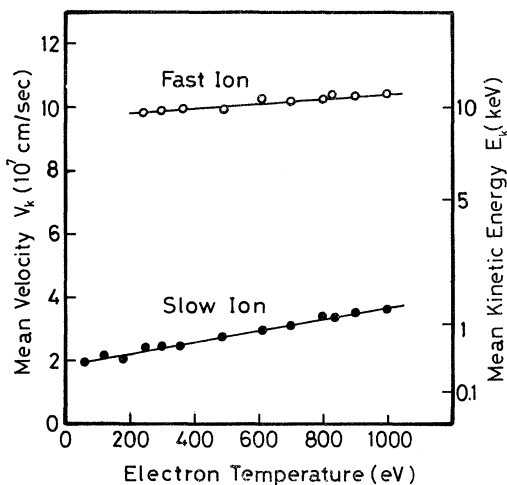


FIG. 7. Dependence of expanding mean velocity  $V_b$  of deuterium plasma on electron temperature.

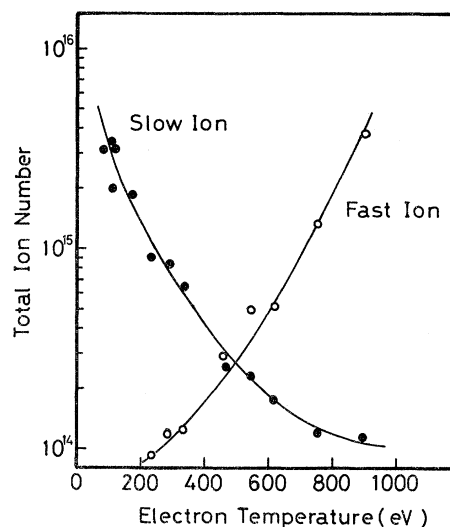


FIG. 8. Ion numbers of fast and slow components vs the electron temperature.

the dependence of the slow component was  $P^{0.3}$ . The appearance of these fast ions exactly corresponded to the appearance of neutrons from the plasma.

The ratio of the energies of the fast ions and the slow ions was 4 to 1 at a laser intensity of  $3 \times 10^{13}$  W/cm<sup>2</sup>, i. e., roughly at the critical point.

#### 4. Neutron Yield

We used three plastic scintillators which were set at distances of 5, 10, and 40 cm from the target to detect the neutrons. The detectors were calibrated using an Am-Be neutron source.

The threshold laser energy for neutron emission was 5 J for a 2-nsec pulse, corresponding to just above the critical intensity of  $10^{13}$  W/cm<sup>2</sup>, and the electron temperature was about 500 eV. With a laser energy of 10 J neutrons were observed in

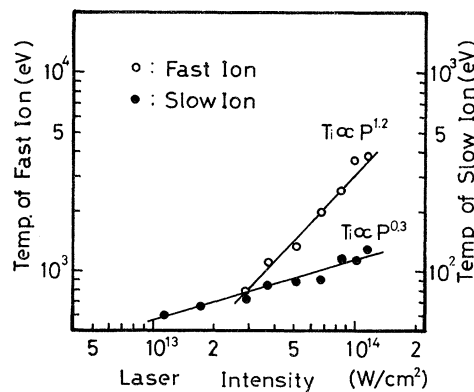


FIG. 9. Dependence of ion temperature  $T_i$  of deuterium plasma on incident laser intensity.

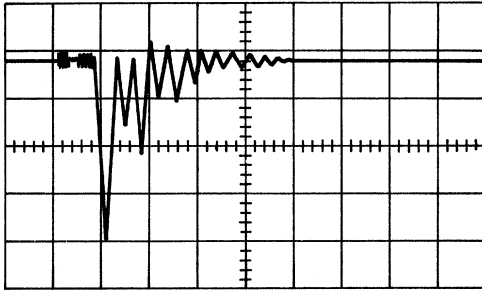


FIG. 10. Neutron yield from solid deuterium irradiated by laser beam. 50 nsec/division. Absorbed laser energy is 5 J.

40% of the shots, and neutrons appeared in every shot when the laser energy was more than 15 J.

The position of the focal spot on the target was very critical for the production of neutrons. Figure 10 shows the response of a plastic scintillator for the neutron flux at the threshold. The dependence of the neutron yield on the absorbed laser energy is shown in Fig. 11. The number of neutrons  $N$  was strongly dependent on the laser energy  $\epsilon$ , varying as  $\epsilon^{4.5}$ . When the number of collected fast ions was about  $10^{15}$ , assuming the ion temperature to be 2.5 keV, then the calculated neutron yield is  $10^4$ , which agrees with the experimental result. There was a close correspondence between the abrupt change of the electron temperature dependence on  $P$ , the appearance of fast ions, and the threshold of the neutron yield. Table II shows a sample of the experimental results leading to this conclusion.

#### IV. DISCUSSION

When a laser pulse, whose duration is larger than a few nsec, is used for plasma production, a hydrodynamic expansion takes place and the energy of the laser is diffused outwards. If a shorter pulse can complete the energy injection into the plasma before the development of the expansion, then we can expect effective heating. The laser energy is mainly supplied to electrons either by

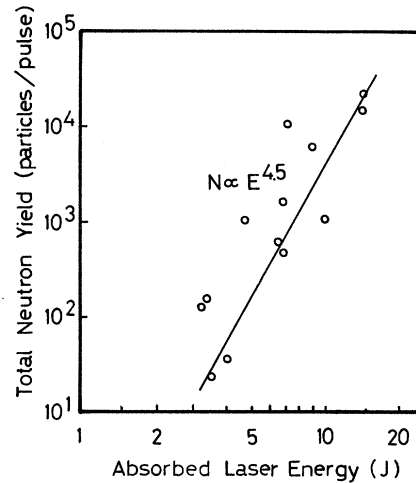


FIG. 11. Dependence of neutron yield on absorbed laser energy.

inverse bremsstrahlung in a collisional plasma or by an anomalous effect in the collisionless state.

In the region of electron temperature less than a few hundred electron volts and for a laser intensity of  $10^{12}$  W/cm<sup>2</sup>, the energy relaxation between electrons and ions is affected by electron-ion collisions. According to the classical theory, the electron-electron relaxation time  $\tau_{ee}$  is  $10^{-13}$  sec and the electron-ion relaxation time  $\tau_{ei}$  is given by

$$\tau_{ei} = \frac{3}{8\sqrt{2}\pi} \frac{m_i T_e^{3/2}}{m_e^{1/2} e^2 z^2 n_e \ln \Lambda}, \quad (1)$$

and the ion transit time  $\tau_s$  is given by

$$\tau_s \approx \frac{x_0}{v_{ac}} = x_0 \left( \frac{5zT_e}{3m_i} \right)^{-1/2}, \quad (2)$$

where  $x_0$  is the plasma dimension, which is of the order of  $10^{-2}$  cm,  $m_e$  and  $m_i$  are the electron and ion masses,  $z$  is the charge,  $n_e$  is the electron density, and  $v_{ac}$  is the sound velocity. When we put  $T_e = 200$  eV,  $n_e = 10^{21}$  cm<sup>-3</sup>, then the values are  $\tau_{ei} \sim 10^{-10}$  sec and  $\tau_s \sim 10^{-9}$  sec. If the initial elec-

TABLE II. Properties of deuterium plasma produced by laser.

Input energy (J)	Electron temperature $T_e$ (keV)	Fast ion		Slow ion		Total neutron yield
		Mean energy $E_k$ (keV)	Temperature (estimated from velocity spread) $T_i$ (keV)	Mean energy $E_k$ (keV)	Temperature (estimated from velocity spread) $T_i$ (eV)	
3	~0.2	...	...	0.7	70	...
5	~0.5	10	1.1	0.9	80	~300
12	~2	11	3.2	1.5	90	~5000
20	~4	~17	~7	2	140	~20000

tron temperature increases,  $\tau_{e1}$  becomes large and relaxation decreases. The electron temperature  $T_e^*$  at  $\tau_{e1} = \tau_s$  gives a condition for relaxation; i. e., for  $T_e^* > T_e$  the ion temperature will approach the electron temperature. For a deuterium plasma  $T_e^*$  has been estimated<sup>23</sup> to be 400 eV. The dependence of the electron temperature on the laser power can be estimated by considering the energy relaxation in the hydrodynamic expansion of the plasma<sup>24</sup> and has been found to be  $T_e \propto P^{2/3}$ . Our experimental results show that this law holds up to a laser intensity of  $10^{13}$  W/cm<sup>2</sup>.

The maximum incident laser intensity was  $10^{14}$  W/cm<sup>2</sup>. At this intensity we may expect anomalous absorption of the laser energy in our experiments. According to the theory of anomalous absorption<sup>25-30</sup> predicted by Nishikawa,<sup>25</sup> two types of instability are expected near  $\omega_0 = \omega_{ep}$ . One is the oscillating two-stream instability, which appears at  $\omega_{ek} > \omega_0$ , where  $\omega_{ek}$  is the Bohm-Gross frequency. The threshold  $P_T$  is given by the following equation:

$$P_T = 2\gamma_e(\omega_{ek} \nu_{ek}/\omega_{ep}^2) n_0 c k T_e \quad (\text{W/cm}^2), \quad (3)$$

where  $\gamma_e$  is compression ratio of the electrons,  $\nu_{ek}$  is the plasma wave damping decrement including electron Landau damping, and  $c$  is the velocity of light.

The other instability is the parametric instability which appears for  $\omega_0 > \omega_{ek}$ . The threshold intensity  $P_p$  is given by the following equation:

$$P_p = \begin{cases} \frac{2\sqrt{3}}{9} \gamma_e \frac{\nu_{ek}^2}{\omega_{ep}} \frac{\nu_{ik}}{\Omega_k^2} n_0 c k T_e \quad (\text{W/cm}^2) & (\nu_{ek} > \Omega_k) \\ \frac{\gamma_e \nu_{ek} \nu_{ik}}{\omega_{ep} \Omega_k} n_0 c k T_e \quad (\text{W/cm}^2) & (\Omega_k > \nu_{ek}), \end{cases} \quad (4)$$

where  $\nu_{ik}$  is the ion acoustic wave damping decrement including ion Landau damping and  $\Omega_k$  is the frequency of ion acoustic wave. We have estimated the threshold for these instabilities in the range of our experiments and these are shown in Fig. 12. For our experimental conditions  $n_0 \approx 10^{21}$  cm<sup>-3</sup>,  $\omega_0 = 1.8 \times 10^{15}$  rad/sec, and Eq. (4) is satisfied in the low-temperature region. This expression has a minimum at  $k\lambda_D = 0.2$ , where  $k$  is the wave number of the instability and  $\lambda_D$  is the Debye shielding distance. The threshold laser intensity decreases with increasing  $T_e$ , varying approximately as  $T_e^{-7/2}$ , since the effective collision frequency of the Landau damping of an ion wave is smaller than the ion-ion collision frequency.

In the high-temperature region, Eq. (5) is satisfied and has a minimum at  $k\lambda_D \approx 0.15$ . In this region the effect of the Landau damping of the ion wave is dominant, the effective collision frequency of the ion wave is independent of temperature (the

value of  $\nu_{ik}$  is about  $4 \times 10^{12}$  Hz), and the threshold laser intensity vary as  $T_e^{-1/2}$ . The threshold of the parametric instability is smaller than that of the oscillating two-stream instability when the electron temperature is larger than 200 eV.

In our experimental conditions the electron temperature was 300 and 400 eV when the laser intensity at the focal point was  $2 \times 10^{13}$  and  $3 \times 10^{13}$  W/cm<sup>2</sup>, respectively. These values almost agree with the calculated value  $10^{13}$  W/cm<sup>2</sup>. Up to an electron temperature of 200 eV, the heating process is mainly controlled by classical absorption, but beyond this temperature the anomalous heating due to the parametric instability seems to dominate. The growth rate of this instability is known to be very fast above threshold<sup>31</sup> and the induced plasma waves tend to saturate and heat the plasma. As shown before, the electron temperature measurement of soft x ray verifies these conclusions. This anomalous effect seems to be very effective in the high-temperature range as shown in Fig. 5. At the threshold of neutron<sup>32</sup> yield we observed the appearance of a fast-ion component as well as the abrupt change of the electron temperature dependence on  $P$ . Concerning the sudden change of the reflection of the laser radiation by the plasma at this critical point, it seems possible that above the threshold the strong laser radiation produces a sharp boundary of very dense plasma, and this induces the strong reflection. While below the threshold the diffused plasma attenuates the re-

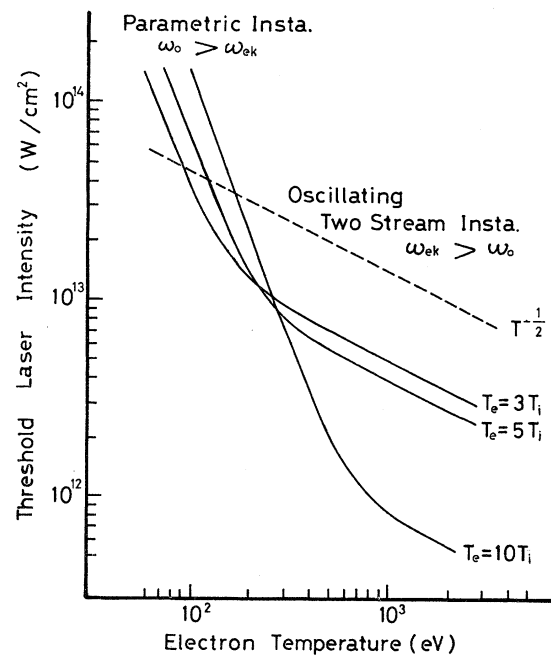


FIG. 12. Estimated threshold laser intensity of oscillating two-stream instability and parametric instability.  $D^+$  plasma,  $n_0 = 10^{21}$  cm<sup>-3</sup>, laser frequency:  $\omega_0 = 1.8 \times 10^{15}$ .

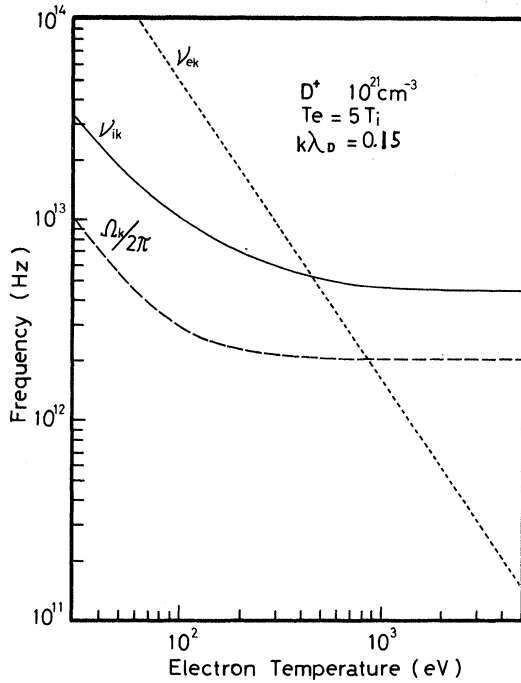


FIG. 13. Wave damping decrement of  $D^+$  plasma and ion acoustic frequency vs electron temperature. Plasma density is  $10^{21} \text{ cm}^{-3}$ ,  $T_e = 5T_i$ , and  $k\lambda_D = 0.15$ .

flected laser beam. The oscillation of reflected light just below the threshold may be due to a macroscopic variation of the plasma surface.

The incident laser energy is mainly taken up by the fast-ion component. The pulse duration of the nanosecond laser has no appreciable influence on the plasma properties at high temperatures.

At the present time experiments are being performed using a picosecond pulse to heat the plasma.

In conclusion, the plasma heating in the keV region, which is a very important subject for laser plasma research, appears to be mainly due to the anomalous absorption of laser light. Also we can say that the threshold intensity of the anomalous heating agrees very well with the theoretical prediction of the onset of the parametric instability of laser radiation and plasma in the hot-electron regime. However, the quantitative distribution of the energy between the electrons and the ions needs to be investigated more thoroughly.

#### ACKNOWLEDGMENTS

The authors wish to thank Dr. K. Nishikawa for stimulating discussion and Dr. Y. Sakagami and N. Miyajima for assistance in performing the experiments. The authors are very grateful to the Toray Science Promotion Society and also to the Ministry of Education for scientific research funds.

Also the authors express their sincere thanks to Professor K. Husimi and Professor K. Takayama of the Institute of Plasma Physics, Nagoya University, for their encouragement.

#### APPENDIX A

In the estimation at high  $\beta$  of the plasma heating, we use the following equations<sup>16</sup>:

$$\left(P - \frac{B^2}{8\pi}\right) 4\pi r^2 \frac{dr}{dt} = \frac{1}{2} \bar{M} \frac{d}{dt} \left(\frac{dr}{dt}\right)^2, \quad (\text{A1})$$

$$P = \frac{3(N_i + N_e)}{4\pi r^3} \kappa T, \quad (\text{A2})$$

$$\frac{3}{2}(N_i + N_e)\kappa \frac{dT}{dt} + \left(P - \frac{B^2}{8\pi}\right) 4\pi r^2 \frac{dr}{dt} = W, \quad (\text{A3})$$

$$W = \begin{cases} \Phi(r/R_0)(1 - e^{-K\nu r}) & (R_0 > r) \\ \Phi(1 - e^{-K\nu r}) & (R_0 < r), \end{cases} \quad (\text{A4})$$

where  $N_i$  and  $N_e$  are the total number of ions and electrons;  $B$  is the applied magnetic field;  $\bar{M}$  is the average plasma mass;  $r$  and  $R_0$  are, respectively, the radius of plasma at time  $t$  and the focal spot of the laser beam;  $P$  is the plasma pressure;  $\kappa$  is the Boltzmann constant;  $T$  is the plasma temperature;  $W$  is the rate of energy absorption by the plasma;  $\Phi$  is the input laser power as a function of time; and  $K_\nu$  is the classical plasma absorption coefficient. A typical solution of these equations is shown in Fig. 3. We assumed that the initial temperature, electron density, and velocity of expansion due to precursor radiation were 10 eV,  $10^{22} \text{ cm}^{-3}$ , and  $2 \times 10^8 \text{ cm/sec}$ , respectively. The laser light was simply absorbed by the classical process, and this solution shows the highest attainable temperature with classical absorption.

#### APPENDIX B

If the plasma has a Maxwellian distribution in energy, the wave damping decrement due to collisional and Landau damping of plasma waves and ion acoustic waves is approximately

$$\nu_{ek} = \nu_{e1} + \frac{1}{2} \pi \frac{\omega_{ep}}{k^3 \lambda_D^3} e^{-1/2k^2 \lambda_D^2}, \quad (\text{B1})$$

$$\nu_{ik} = \nu_{i1} + \frac{1}{8} \pi \Omega_k \left(\frac{zT_e}{T_i}\right)^{3/2} e^{-zT_e/2T_i} \quad (T_e \gg T_i), \quad (\text{B2})$$

where  $\nu_{e1}$  and  $\nu_{i1}$  are the collision frequency between electron-ion and ion-ion, respectively,  $T_e$  and  $T_i$  are the electron and ion temperature, and  $z$  is the average charge of the ions. In equation (B2), the Landau damping caused by the electrons

has been neglected. The values of these under our experimental condition are shown in Fig. 13. The solid and dotted curves are, respectively, the wave

damping decrement of ion acoustic waves and that of plasma waves. The dashed curve is the frequency of ion acoustic waves.

\*Guest staff of Institute of Plasma Physics, Nagoya University, Nagoya, Japan.

<sup>1</sup>N. G. Basov, P. G. Kriukov, S. D. Zakharov, Yu. V. Senatsky, and S. V. Tchekalin, *IEEE J. Quantum Electron.* **QE-4**, 864 (1968).

<sup>2</sup>F. Floux, D. Cognard, L. -G. Denoeud, G. Piar, D. Parisot, J. M. Bobin, F. Delobbeau, and C. Fauquignon, *Phys. Rev. A* **1**, 821 (1970).

<sup>3</sup>C. Yamanaka, T. Yamanaka, T. Sasaki, H. Kang, K. Yoshida, and M. Waki, in *International Quantum Electronics Conference, Kyoto, 1970, Digest of Technical Papers*, p. 16 (unpublished); *Proceedings of the International Conference on Laser Plasma, Moscow, 1970* (unpublished).

<sup>4</sup>T. Sasaki, T. Yamanaka, G. Yamaguchi, and C. Yamanaka, *Japan J. Appl. Phys.* **8**, 1037 (1969).

<sup>5</sup>C. Yamanaka, T. Yamanaka, and T. Sasaki, in *International Quantum Electronics Conference, Kyoto, 1970, Digest of Technical Papers*, p. 404 (unpublished).

<sup>6</sup>K. Yoshida, T. Yamanaka, T. Sasaki, H. Kang, M. Waki, and C. Yamanaka, *Japan J. Appl. Phys.* **10**, 1643 (1971).

<sup>7</sup>C. Yamanaka, T. Sasaki, M. Hongyo, and Y. Nagao, in *Proceedings of the Conference on Damage in Laser Materials, Boulder, 1971* (unpublished); *ASTN Damage in Laser Materials*, edited by A. J. Glass and A. Guenther (National Bureau of Standards, Boulder, Colo., 1971), p. 104.

<sup>8</sup>C. Yamanaka, T. Sasaki, and M. Hongyo, *IEEE J. Quantum Electron.* **QE-7**, 291 (1971).

<sup>9</sup>M. Ohnishi and C. Yamanaka, *Tech. Rept. Osaka Univ.* **20**, 121 (1970).

<sup>10</sup>P. Langer, G. Tonon, F. Floux, and A. Ducauge, *IEEE J. Quantum Electron.* **QE-2**, 499 (1966).

<sup>11</sup>B. C. Boland, F. E. Irons, and R. W. P. McWhirter, *J. Phys. B* **1**, 1180 (1968).

<sup>12</sup>B. E. Patron and N. R. Isenor, *Can. J. Phys.* **46**, 1237 (1968).

<sup>13</sup>M. Mattioli and D. Véron, *Plasma Phys.* **11**, 684 (1969).

<sup>14</sup>W. Demtröder and W. Jantz, *Plasma Phys.* **12**, 691 (1970).

<sup>15</sup>C. Yamanaka and T. Yamanaka, *Progress Reports of Plasma Electronics, Osaka University, 1968* (unpublished).

<sup>16</sup>A. F. Haught and D. H. Polk, *Phys. Fluids* **9**, 2047 (1966).

<sup>17</sup>T. Yamanaka and C. Yamanaka, *Tech. Rept. Osaka Univ.* **18**, 155 (1968).

<sup>18</sup>J. A. Stamper *et al.*, *Phys. Rev. Letters* **26**, 1012 (1971).

<sup>19</sup>Y. Izawa and C. Yamanaka, *Japan J. Appl. Phys.* **7**, 954 (1968).

<sup>20</sup>M. Waki, T. Yamanaka, H. Kang, K. Yoshida, and C. Yamanaka, *Japan J. Appl. Phys.* **11**, 420 (1972).

<sup>21</sup>H. Kang, T. Yamanaka, K. Yoshida, M. Waki, and C. Yamanaka, *Japan J. Appl. Phys.* **11**, 765 (1972).

<sup>22</sup>F. J. Allen, *J. Appl. Phys.* **14**, 3048 (1970).

<sup>23</sup>N. G. Basov *et al.*, *Quantum Radiophysics Laboratory Preprint No. 60, 1970* (unpublished).

<sup>24</sup>C. Fauquignon and F. Floux, *Phys. Fluids* **13**, 386 (1970).

<sup>25</sup>K. Nishikawa, *J. Phys. Soc. Japan* **24**, 916 (1968); **24**, 1152 (1968).

<sup>26</sup>C. Yamanaka *et al.*, *Phys. Letters* **38A**, 495 (1972).

<sup>27</sup>E. A. Jackson, *Phys. Rev.* **153**, 235 (1967).

<sup>28</sup>P. K. Kaw, E. Valeo, and J. M. Dawson, *Phys. Rev. Letters* **25**, 430 (1970).

<sup>29</sup>E. Valeo, C. Oberman, and F. W. Perkins, *Phys. Rev. Letters* **28**, 340 (1972).

<sup>30</sup>D. F. DuBois and M. V. Goldman, *Phys. Rev. Letters* **28**, 218 (1972).

<sup>31</sup>P. Kaw, J. Dawson, W. Kruer, C. Oberman, and E. Valeo, *Princeton University, Institute of Plasma Physics, Report No. Matt-817, 1970* (unpublished).

<sup>32</sup>C. Yamanaka, T. Yamanaka, T. Sasaki, K. Yoshida, M. Waki, and H. B. Kang, *Institute of Plasma Physics Nagoya University Research Report No. IPPJ-117, 1972* (unpublished).